This is the post-print (i.e. final draft post-refereeing) of the publication.
The final publication is available at Wiley Online Library via http://dx.doi.org/10.1111/jace.13417

Microstructural features and functional properties of bilayered $BaTiO_3/BaTi_{1-x}Zr_xO_3$ ceramics

Thiago Martins Amaral[‡1], Eduardo Antonelli[¶], Diego Alejandro Ochoa[§], José Eduardo García[§], Antonio Carlos Hernandes[‡]

[‡] *Grupo de Crescimento de Cristais e Materiais Cerâmicos, Physics Institute of São Carlos, University of São Paulo, 13560-970 São Carlos, SP, Brazil*

[§] *Department of Applied Physics, Universitat Politècnica de Catalunya – BarcelonaTech, 08034 Barcelona, Spain*

[¶] *Science and Technology Institute, Federal University of São Paulo - UNIFESP, São José dos Campos, SP, Brazil*

Abstract

Validity of mixture rule for dielectrics in series configuration and the correlation between microstructure and electrical properties in bilayered $BaTiO_3/BaTi_{1-x}Zr_xO_3$ ceramics were studied. Samples were obtained from $BaTi_{1-x}Zr_xO_3$ (BTZx) nanopowder synthesized by the polymeric precursor technique and had their microstructure, dielectric, piezoelectric and ferroelectric properties investigated. These bilayered ceramics properties were compared to the properties of homogeneous BTZx samples. And, also, the former's electrical permittivities were compared with the predictions of the simple mixture rule. According to the results, the microstructures of the layers do not differ from the microstructure of the corresponding homogeneous BTZx ceramic. And pyroelectric coefficient measurements show that the electrical properties of the interface do not contribute to the functional properties of the bilayered samples. Nevertheless, on increasing Zr^{4+}, the agreement between the experimental and the predicted permittivity of the

[1] thimaral@ursa.ifsc.usp.br

bilayered ceramics is gradually reduced, mainly at temperatures where the permittivity is governed by the response of the layer containing Zr^{4+}. As a mechanical joint between the layers, the interface induces stresses during sintering due to thermal mismatch between compositions, thereby affecting the bilayer's electrical properties. Our results show that mechanical interface effects compromise the functional properties of layered ferroelectric ceramics.

I. Introduction

Barium titanate ($BaTiO_3$) is a perovskite type (ABO_3) ferroelectric material that has been known since the 1940s.[1] However, it still attracts much attention as a promising and environmentally friendly material for a variety of electronic devices such as capacitors, memory storage systems, piezoelectric, pyroelectric and microwave components.[2,3] In fact, $BaTiO_3$ is nowadays the base material for most capacitors,[4,5] particularly for multi-layer ceramic capacitors (MLCC). In order to meet the technological requirements that these capacitors must satisfy, i.e. high electrical permittivity, low dielectric loss and temperature stability of properties, $BaTiO_3$ must be modified.[6] Among the possible modifications, the substitution of Ti^{+4} ion by the larger ionic radius Zr^{+4} in the B-site leads to the solid solution compound $BaTi_{1-x}Zr_xO_3$ (BTZx).[7] When compared to the $BaTiO_3$, this solid solution has reduced dielectric losses due to the higher chemical stability of the Zr^{4+} ion. And, furthermore, the Curie temperature of the BTZ system gradually decreases as the zirconium content increases, while (for Zr^{4+} substitutions greater than 15 %) the electrical permittivity peak broadens in temperature due to an increase in the diffusive character of the ferroelectric to paraelectric phase transition.[8–10]

A way to increase the range of temperature stability in capacitors was explored by Ota *et. al.*, by means of the mixture rules, to design capacitors from laminar bulk ceramics with layers of $Ba_{1-x}Sr_xTiO_3$ [11] and (1-x)$PbMg_{1/3}Nb_{2/3}O_3$-x$PbTiO_3$ [12]. These mixture rules, reunited in 1986 by Newham [13], predict the properties of a composite based on the properties and volumetric fractions of its linear, isotropic and homogeneous components. Other works also turned their attention to studying laminar bulk ceramics of perovskite compounds. For instance, Gopalan *et al.* focused their research on ionic transport and vacancy generation through the interface between $BaTiO_3$-$SrTiO_3$ diffusion couples [14] and between layers of $BaTi_{0.7}Zr_{0.3}O_3$ and $BaTi_{0.3}Zr_{0.7}O_3$ [15]. Furthermore, Siao *et al.* [16] studied inter-diffusion and Kirkendall porosity in bilayered $BaTiO_3$/$SrTiO_3$ ceramics, while Maurya et al. [17] studied the piezoelectric and ferroelectric properties of layered $BaTiO_3$/0.975$BaTiO_3$-0.025$Ba(Cu_{1/3}Nb_{2/3})O_3$ ceramics. Nevertheless, none of these authors considered the correlations between microstructural features of these bulk layered ceramics and their functional properties, e.g. the correlation between the interface characteristics and the electrical properties.

The aim of the present work is to investigate microstructural, dielectric, ferroelectric, and piezoelectric properties of bilayered bulk $BaTiO_3$/$BaTi_{1-x}Zr_xO_3$ ceramics. Special interest is given to the correlation between their microstructure and functional properties. And validation of the mixture rule for this system is also investigated, with the aim of making a tool available for designing more complex $BaTiO_3$-based layered ceramics for specific demands.

II. Experimental Procedure

$BaTi_{1-x}Zr_xO_3$ (x=0, 0.05, 0.1 and 0.15) powders were produced using the polymeric precursor route with Barium acetate (99%, Alpha Aesar), Ti(IV)-isopropoxide (97%, Sigma Aldrich), Zr(IV)-propoxide solution (70% Sigma Aldrich), citric acid (99.5%, Synth) and ethylene glycol (99.5%, Synth) [18]. $BaTi_{1-x}Zr_xO_3$ (x=0, 0.05, 0.1 and 0.15) dense ceramics and bilayered $BaTiO_3/BaTi_{0.95}Zr_{0.05}O_3$, $BaTiO_3/BaTi_{0.9}Zr_{0.1}O_3$ and $BaTiO_3/BaTi_{0.85}Zr_{0.15}O_3$ ceramics were prepared by uniaxially pressing the powders under 30 MPa, one layer above the other, should that be the case, and then isostatically pressing at 350 MPa to produce disc-shaped samples (6 mm diameter and 1 mm thick). Then, the pellets were sintered at 1300 °C for 2 h.

The microstructure was analyzed by scanning electron microscopy (SEM) (Inspect F-50, FEI, Hillsboro, USA). The atomic concentration profile was obtained from line scan energy dispersive X-ray spectroscopy (EDX). The results from EDX analysis were used to confirm stoichiometry and estimate the interface and layer thicknesses and the volumetric fraction of each composition on the bilayered ceramics.

Samples electrodes were sputtered with gold for dielectric, ferroelectric and piezoelectric measurements. The dielectric permittivity was measured in non-polarized samples from room temperature to 150 °C with rate of 1 °C/min (FRA SI 1260 with dielectric interface 1296A, Solartron Analytical - Ametek, New York, USA). For the other measurements, samples were poled in an oil bath by applying an electric field of 2.0 kV/mm for 30 min at 25 °C. The longitudinal piezoelectric coefficient is measured using a piezo-d_{33} meter (PM3500, KCF Technologies, State College, USA) at room temperature. The pyroelectric coefficient was evaluated from the thermally stimulated depolarization current, measured by a Sub-

Femtoamperimeter (Model 6430, Keithley, Cleveland, USA) at a heating rate of 5 °C/min.

The relative thermal expansion of the homogeneous samples was measured in a dilatometer (DIL 402 PC, NETZSCH, Selb, Germany) under a thermal treatment equal to the sintering treatment. Results obtained during cooling from 1200 °C to room temperature, and the reported value of the $BaTiO_3$'s Young Modulus (67 GPa [19]), were used to estimate stress of the bilayered samples due to thermal mismatch between the layers.

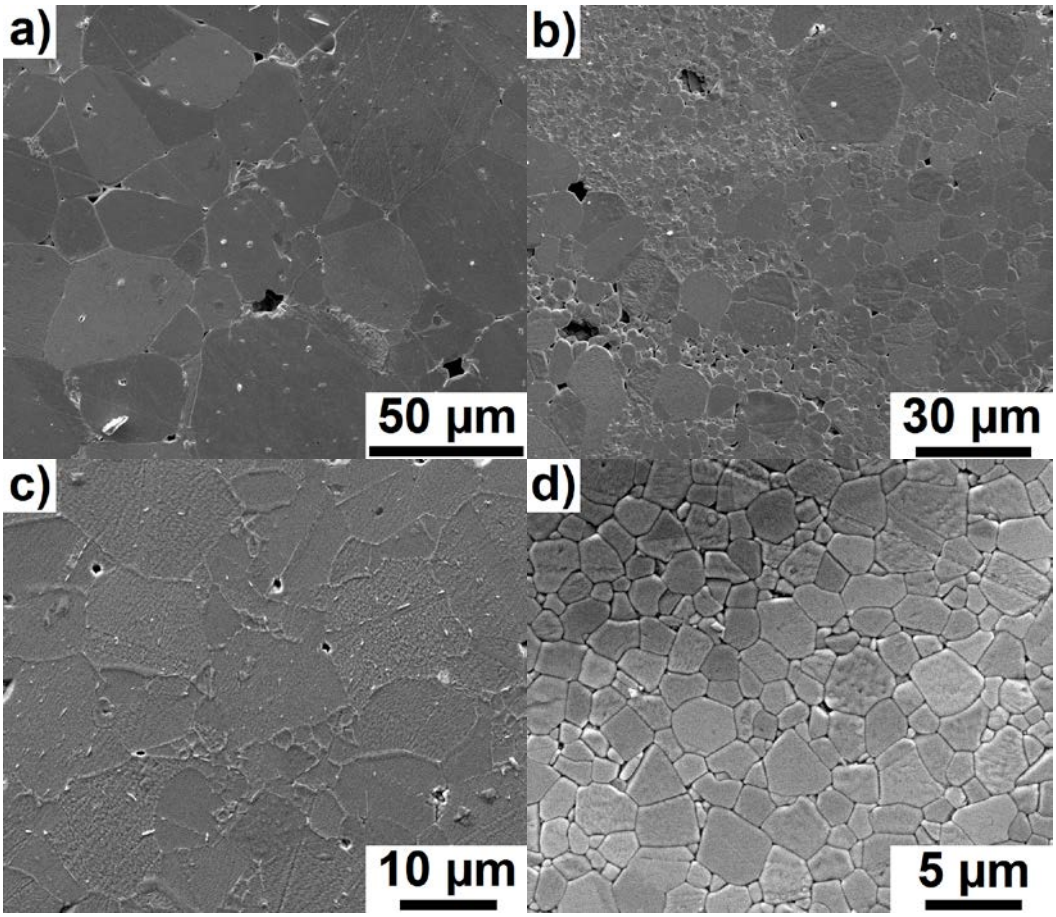

Fig. 1. SEM micrographs of homogeneous **a)** $BaTiO_3$, **b)** $BaTi_{0.95}Zr_{0.05}O_3$, **c)** $BaTi_{0.9}Zr_{0.1}O_3$, and **d)** $BaTi_{0.85}Zr_{0.15}O_3$ ceramics.

III. Results and Discussion

(1) $BaTi_{1-x}Zr_xO_3$ ceramics

Scanning electron microscopy micrographs of $BaTi_{1-x}Zr_xO_3$ ceramics are shown in Figure 1 a)-d). As Zr^{4+} substitution for Ti^{4+} increases, the average grain size decreases from 33 µm in $BaTiO_3$ to less than 2 µm in $BaTi_{0.85}Zr_{0.15}O_3$, presumably due to the slowest diffusion rate of Zr^{4+}, inhibiting grain growth [20]. $BaTi_{0.95}Zr_{0.05}O_3$ has bimodal grain size distribution with average diameters of 13 and 2 µm, and $BaTi_{0.9}Zr_{0.1}O_3$ has an average grain size of 12 µm. No secondary phase or segregation is detected in grain boundaries.

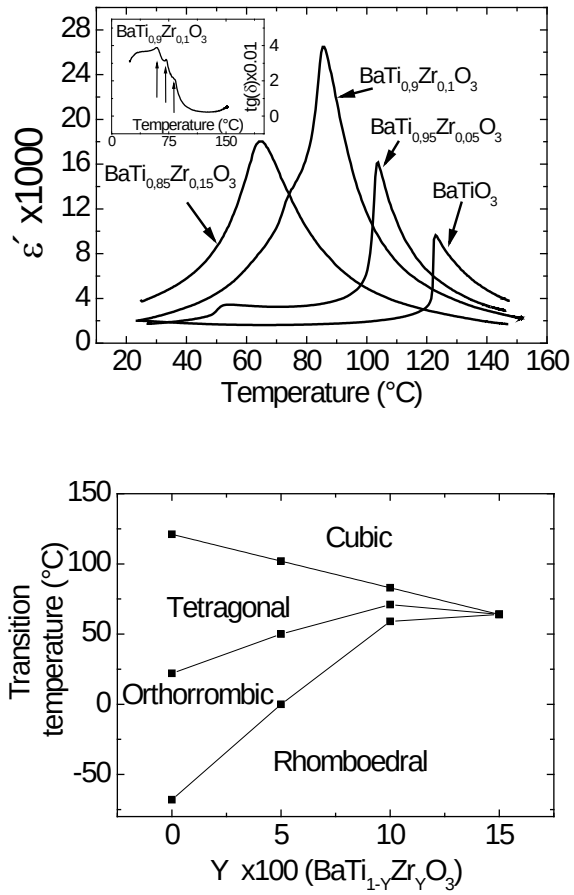

Fig. 2. a) Temperature-dependent real permittivity of homogeneous $BaTi_{1-x}Zr_xO_3$ (x=0, 0.05, 0.1 and 0.15) samples and; **b)** phase transition temperatures evaluated by dielectric response. Temperature-dependent dielectric loss of $BaTi_{0.9}Zr_{0.1}O_3$ is shown in the inset of **a)**.

Figure 2 a) shows the dielectric permittivity data at 1 kHz of $BaTi_{1-x}Zr_xO_3$ ceramics for temperatures from 25 to 150 °C. In this range of temperature, it is possible to observe: the tetragonal-to-cubic phase transition of the $BaTiO_3$; the orthorhombic-to-tetragonal and the tetragonal-to-cubic phase transitions of the $BaTi_{0.95}Zr_{0.05}O_3$; the rhomboedral-to-orthorhombic, the orthorhombic-to-tetragonal and the tetragonal-to-cubic phase transitions of the $BaTi_{0.9}Zr_{0.1}O_3$ smeared out in the observable real permittivity peak; and the pinched rhombohedral-to-cubic phase transition of the $BaTi_{0.85}Zr_{0.15}O_3$. The $BaTi_{0.9}Zr_{0.1}O_3$ phase transitions are better resolved in the dielectric loss temperature dependence of this composition, as shown in the inset. These dielectric permittivities versus temperature data are used as input to the mixture rule in order to predict real dielectric permittivity values for the bilayered ceramics.

Figure 2 b) summarizes in a phase diagram the phase transition temperatures obtained for each $BaTi_{1-x}Zr_xO_3$ ceramic. On increasing Zr^{4+} substitution of Ti^{4+}, there is a gradual decrease in the Curie temperature and an increase in the temperatures of the other phase transitions. For 15% of Zr^{4+} substitution, the three phase transitions merge together in a pinched phase transition, as also reported by other authors [10]. The difference between the ionic radius of Zr^{4+} and Ti^{4+}, when the former substitutes the latter, leads to a depressed displacement of Zr^{4+} in B-site of the O^{2-} octaedra and to a weaker bonding with O^{2-}. This results in a “break” of the cooperative vibrations of the B-O chains responsible for ferroelectricity in $BaTiO_3$, which manifests itself macroscopically in the decrease of the Curie temperature and changes in the ferroelectric and piezoelectric properties of the $BaTi_{1-x}Zr_xO_3$ compounds [21, 22].

Table I. Remanent polarization (P_r), coercive field (E_c), and piezoelectric coefficient (d_{33}) values obtained for homogeneous $BaTi_{1-x}Zr_xO_3$ ceramics. Values from other authors are also reported.

Composition	P_r (μC/cm²) ± 0.3		E_c(kV/mm) ± 0.2		d_{33}(pC/N) ± 5	
$BaTiO_3$	9.8	5.45[23]	3.8	3.14[23]	130	190 [2]
$BaTi_{0.95}Zr_{0.05}O_3$	7.9	6.7[21], 13.3[8], 9.0[24], 5.4[25]	3.6	4.8[21], 3.5[8], 3.3[24], 1.86[25]	162	91[8], 208[24]
$BaTi_{0.9}Zr_{0.1}O_3$	6.8	7[21], 6.2[24], 5.3[25]	2.6	5.8[21], 2.4[24], 1.34[25]	120	160[24]
$BaTi_{0.85}Zr_{0.15}O_3$	4.5	5.4[21], 2.0[8], 3.1[24], 3.6[25]	1.5	0.22[21], 1.3[8], 1.8[24], 1.5[25]	70	82[8], 150[24]

Table I summarizes the remanent polarization (P_r), the coercive field (E_c) and the piezoelectric coefficient (d_{33}) for the $BaTi_{1-x}Zr_xO_3$ ceramics at 25 °C. Values obtained by other authors [2, 8, 21, 23–25] are included for comparison. The substitution of Ti^{4+} for Zr^{4+} hardens the ceramics and reduces their ferroelectric and piezoelectric properties. The $BaTi_{0.95}Zr_{0.05}O_3$ composition is an exception, because it presents its orthorhombic-to-tetragonal phase transition close to room temperature, maximizing their properties as a consequence of the polarization extension phenomenon [26].

(2) Bilayered $BaTiO_3$/$BaTi_{1-x}Zr_xO_3$ ceramics

Figure 3 a)-c) shows SEM micrographs of bilayered $BaTiO_3$/$BaTi_{1-x}Zr_xO_3$ ceramics together with their Zr concentration profile, their interface thickness and the volumetric fraction of each layer. Far from the interface, the layers have no microstructural and no chemical differences when compared to the corresponding homogeneous $BaTi_{1-x}Zr_xO_3$ ceramic, presenting the same average grain size (including bimodal grain size distribution in the $BaTi_{0.95}Zr_{0.05}O_3$ layer) and same composition. As the thicknesses of the layers are wider than the length of many grains, isotropic crystalline orientation of each layer is expected [13]. And no second phase segregation on grain boundary was detected. The interface, i.e. the region between layers, is characterized by a change in Zr^{4+} concentration with length and by a remanent porosity from material processing (also reported by other authors in

bilayered $BaTiO_3/SrTiO_3$ ceramics [16]). The interfaces of the $BaTiO_3/BaTi_{0.95}Zr_{0.05}O_3$ and $BaTiO_3/BaTi_{0.9}Zr_{0.1}O_3$ samples were observed to be thicker than that of the $BaTiO_3/BaTi_{0.85}Zr_{0.15}O_3$, probably because of the sizes of the grains in each adjacent layer that are available for coalescence processes during sintering. Table II summarizes the remanent polarization (P_r), the coercive field (E_c) and the piezoelectric coefficient (d_{33}) for bilayered $BaTiO_3/BaTi_{1-x}Zr_xO_3$ ceramics at 25 °C. It is observed that the bilayered samples show intermediate ferroelectric and piezoelectric properties when compared to the corresponding homogeneous $BaTi_{1-x}Zr_xO_3$ ceramics. The fact that this layered design of ferroelectric ceramics doesn't improve properties related to remanent polarization was already reported [17] and it happens because of depolarizing fields at the interface between the layers [27].

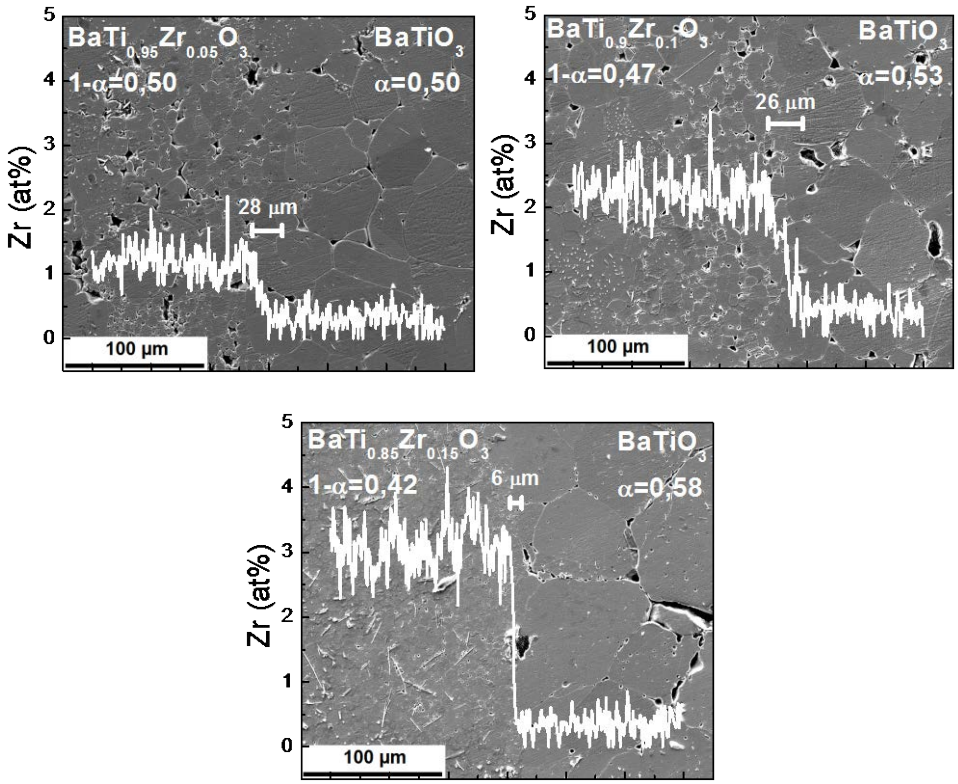

Fig. 3. SEM micrograph of bilayered **a)** $BaTiO_3/BaTi_{0.95}Zr_{0.05}O_3$, **b)** $BaTiO_3/BaTi_{0.9}Zr_{0.1}O_3$ and **c)** $BaTiO_3/BaTi_{0.85}Zr_{0.15}O_3$ ceramics. The composition, volumetric fraction (α) and interface thickness of each layer are displayed. Zirconium concentration profiles as a function of the longitudinal length are linked in the micrographs.

Table II. Remanent polarization (P_r), coercive field (E_c), piezoelectric coefficient (d_{33}) values and estimated maximum stress in $BaTiO_3$ layer due to thermal mismatch (σ) for the bilayered $BaTiO_3$/ $BaTi_{1-x}Zr_xO_3$ ceramics.

Sample	P_r (μC/cm^2)±0.3	E_c(kV/mm) ±0.2	d_{33}(pC/N) ±5	σ(MPa)
$BaTiO_3/BaTi_{0.95}Zr_{0.05}O_3$	8.9	3.4	123	8
$BaTiO_3/BaTi_{0.9}Zr_{0.1}O_3$	9.5	2.6	111	102
$BaTiO_3/BaTi_{0.85}Zr_{0.15}O_3$	8.4	2.1	98	164

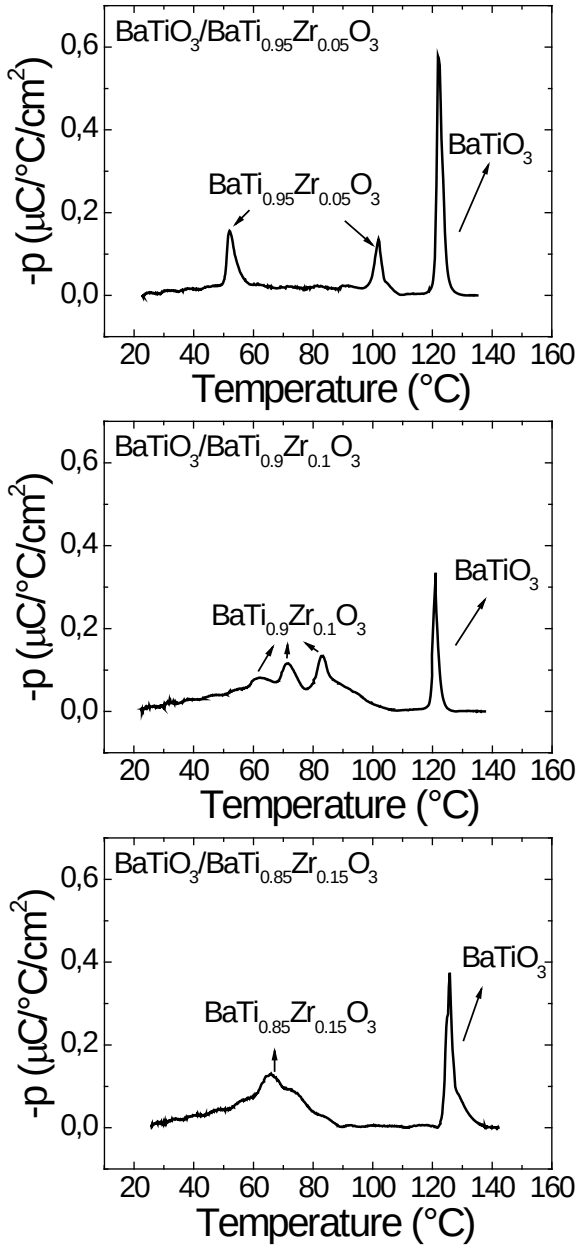

Fig. 4. Temperature-dependent pyroelectric coefficient of bilayered **a)** $BaTiO_3/BaTi_{0.95}Zr_{0.05}O_3$, **b)** $BaTiO_3/BaTi_{0.9}Zr_{0.1}O_3$ and **c)** $BaTiO_3/BaTi_{0.85}Zr_{0.15}O_3$ ceramics identifying peaks corresponding to phase transitions of each layer composition.

Figure 4 shows the temperature dependence of the pyroelectric coefficient for bilayered $BaTiO_3/BaTi_{1-x}Zr_xO_3$ ceramics. For x=0.05 (Figure 4-a)), the pyroelectric coefficient has three peaks around 50 °C, 103 °C and 123 °C, respectively, related to the transitions of the $BaTi_{0.95}Zr_{0.05}O_3$ and the transition of the $BaTiO_3$. For x=0.1 (Figure 4-b)), the pyroelectric coefficient has four peaks associated with the transitions of the $BaTi_{0.9}Zr_{0.1}O_3$ at 60°C, 70 °C and 82 °C, and the transition of the $BaTiO_3$ at 123 °C. The pyroelectric coefficient of $BaTiO_3/BaTi_{0.85}Zr_{0.15}O_3$ (Figure 4-c)) has two peaks, related to the pinched diffuse transition of the $BaTi_{0.85}Zr_{0.15}O_3$ around 65 °C and to the ferroelectric-to-paraelectric phase transition of the $BaTiO_3$ at 123 °C. The sharp observed peaks, associated with the layers of $BaTiO_3$, $BaTi_{0.95}Zr_{0.05}O_3$ and $BaTi_{0.9}Zr_{0.1}O_3$, contrast with the broad peak associated with the $BaTi_{0.85}Zr_{0.15}O_3$ layer due to the diffuse character of the pinched phase transition of this last compound [9]. The temperature dependence of the pyroelectric coefficient presents no other signal besides those of the compositions of each layer, probably due to the small interface thickness when compared with the dimensions of the samples.

Figure 5 shows the temperature dependence of the real permittivity of the studied bilayered $BaTiO_3/BaTi_{1-x}Zr_xO_3$ ceramics together with the predicted values obtained by the simple mixture rule. The volumetric fractions (α and $1-\alpha$) of each $BaTi_{1-x}Zr_xO_3$ layer and the temperature dependence of the permittivities (ε_1 and ε_2) of homogeneous samples fed the mixture rule, with the purpose of predicting the permittivity of the heterostructure (ε), according to the following equation for serial configuration:

$$\frac{1}{\varepsilon} = \frac{\alpha}{\varepsilon_1} + \frac{1-\alpha}{\varepsilon_2}.$$

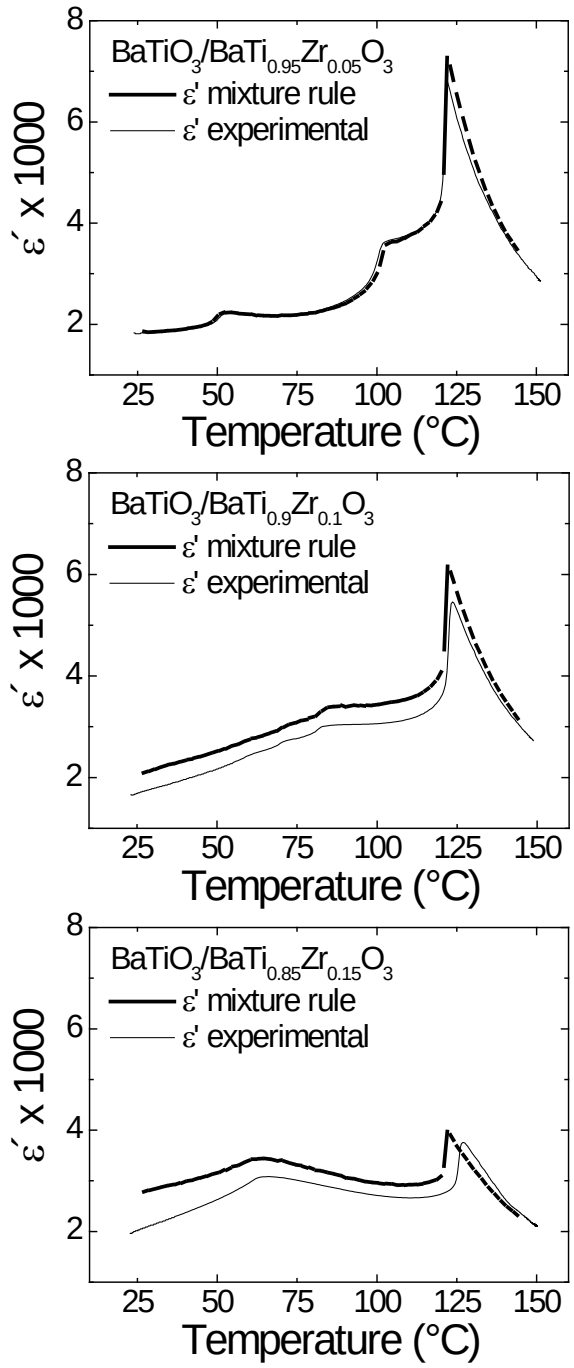

Fig. 5. Experimental and predicted temperature-dependent real permittivity of bilayered **a)** $BaTiO_3/BaTi_{0.95}Zr_{0.05}O_3$, **b)** $BaTiO_3/BaTi_{0.9}Zr_{0.1}O_3$, and **c)** $BaTiO_3/BaTi_{0.85}Zr_{0.15}O_3$ ceramics.

As in the temperature dependence of the pyroelectric coefficient (Figure 4), it is also possible to associate each permittivity peak of the bilayered ceramics displayed in Figure 5 with the composition of each layer. Figure 5-a) shows the real permittivity of

$BaTiO_3/BaTi_{0.95}Zr_{0.05}O_3$, where the peaks correspond to the two observable phase transitions of the $BaTi_{0.95}Zr_{0.05}O_3$ layer and to the one observable phase transition of the $BaTiO_3$ layer at 52 °C, 102 °C, and 122 °C, respectively. Figure 5-b) shows the real permittivity of $BaTiO_3/BaTi_{0.9}Zr_{0.1}O_3$, where the three peaks correspond to the phase transitions of the $BaTi_{0.9}Zr_{0.1}O_3$ layer and to that of the $BaTiO_3$ layer at 60 °C, 70 °C, 83 °C, and 123 °C, respectively. And the real permittivity of $BaTiO_3/BaTi_{0.85}Zr_{0.15}O_3$ is displayed in Figure 5-c), where the peak corresponding to the diffuse phase transitions of the $BaTi_{0.85}Zr_{0.15}O_3$ layer can be identified as well as that of the $BaTiO_3$ layer at 66 °C and 123 °C, respectively.

It is observed that, in the temperature range where phase transitions of $BaTi_{0.9}Zr_{0.1}O_3$ take place (i.e. around 60 °C and 90 °C), the permittivity peaks (Figure 5-b) are smoothed out, while the pyroelectric peaks (Figure 4-b) are sharp peaks. When designing permittivity versus temperature profiles, a smoothed dielectric response is expected when ferroelectric/ferroelectric transitions are close one to the other with respect to temperature. However, a sharp pyroelectric peak appears in a phase transition when the polarization suddenly changes in order to adapt to the new unit cell of the material. And also it is expected that, in the temperature range between phase transitions, scarce pyroelectric response will occur due only to thermal depolarization.

The predictions for the electrical permittivity by the simple mixture rule sufficiently agree with the experimental results for the studied samples, which means that the unpoled bilayered ceramics may be regarded as isotropic, homogeneous and linear media while 1 V/mm is applied, and that many layers of different $BaTi_{1-x}Zr_xO_3$ compositions could be stacked together in specific volumetric fractions in order to design a desired electrical permittivity temperature profile, as done by Ota *et. al* with

other compositions [11, 12]. Nevertheless, two features should be pointed out while analyzing Figure 5; firstly, there is an increase in the disagreement between experimental and predicted permittivities on increasing Zr^{4+} content in one of the layers, and secondly, the experimental values deviate more from the predicted in temperatures where the phase transitions of the $BaTi_{1-x}Zr_xO_3$ layer occur. These observations concerning mixture rule validity under low electrical field can be explained by assuming that the interface introduces stress while playing a mechanical joint role during co-sintering of the layers. Other authors[17] also assumed that stresses were present in their bilayered and trilayered samples .

The estimated stresses in the $BaTiO_3$ layer due to thermal mismatch on the studied samples are shown in the last column of Table II. As, it is accepted that there is a stress gradient on the samples, these values would correspond to the maximum stress present [28]. And it is known that phase transition temperatures and ferroelectric and piezoelectric properties of $BaTiO_3$ are affected by stresses [29–33]. Then, on one hand, it is observed that stress increases as Zr^{+4} substitution increases in the sample's $BaTi_{1-x}Zr_xO_3$ ($x \neq 0$) layer. And, on the other hand, a recent work [34] observed that Zr^{4+} substitution in $BaTiO_3$ ceramics makes their properties more susceptible to stress. So, in bilayered $BaTiO_3/BaTi_{0.95}Zr_{0.05}O_3$ ceramics, there is less Zr^{4+} and the smallest observed stress, thus, not compromising electrical properties or the validity of the simple mixture rule. Nevertheless, with further increase in Zr^{4+} content, the stress on the samples increases and the samples become more susceptible to the stress effects. Thus, their functional properties are compromised and validity of simple mixture rule is gradually lost, mainly where the contribution from $BaTi_{1-x}Zr_xO_3$ ($x \neq 0$) layer on the electrical permittivity is greater than the

$BaTiO_3$'s contribution, as observed, for example, close to the phase transitions temperatures of $BaTi_{1-x}Zr_xO_3$ ($x \neq 0$).

IV. Conclusions

Microstructure, piezoelectric, ferroelectric and dielectric properties of the bilayered $BaTiO_3/BaTi_{1-x}Zr_xO_3$ ceramics are reported, correlated and compared with properties of homogeneous $BaTi_{1-x}Zr_xO_3$ samples. The interface joined the layers together, constraining the sintering process and inducing stress due to thermal mismatch between compositions. When there is small thermal mismatch stresses, it was shown that these layered ceramics could be used to smooth permittivity temperature behavior and that the mixture rule predictions holds for bilayered $BaTiO_3/BaTi_{1-x}Zr_xO_3$ ceramics. Nevertheless, as the Ti^{4+} substitution increases, mixture rule predictions gradually lacked experimental correspondence due to increase in thermal mismatch stress and increase of the stresses effects over the properties of the $BaTi_{1-x}Zr_xO_3$ layers.

Acknowledgments

The authors gratefully acknowledge financial support from FAPESP and CNPq, two Brazilian research-funding agencies. Support from the project MAT2013-48009-C4-2-P of the Spanish Government is also appreciatively acknowledged.

References

[1] G.H. Haertling, “Ferroelectric Ceramics: History and Technology,” *J. Am. Ceram. Soc.*, **82** [4] 797–818 (1999).

[2] T.R. Shrout and S.J. Zhang, “Lead-free piezoelectric ceramics: Alternatives for PZT?,” *J. Electroceramics*, **19** [1] 111–124 (2007).

[3] T. Karaki, K. Yan, T. Miyamoto, and M. Adachi, “Lead-Free Piezoelectric Ceramics with Large Dielectric and Piezoelectric Constants Manufactured from BaTiO 3 Nano-Powder,” *Jpn. J. Appl. Phys.*, **46** [No. 4] L97–L98 (2007).

[4] H. Kishi, Y. Mizuno, and H. Chazono, “Base-Metal Electrode-Multilayer Ceramic Capacitors: Past, Present and Future Perspectives,” *Jpn. J. Appl. Phys.*, **42** [Part 1, No. 1] 1–15 (2003).

[5] A.C. Randall, “Scientific and Engineering Issues of the State-of-the-Art and Future Multilayer Capacitors,” *J. Ceram. Soc. Japan*, **109** [1] 2–6 (2001).

[6] H.-W. Lee, M.S.H. Chu, and H.-Y. Lu, “Phase Mixture and Reliability of BaTiO3-Based X7R Multilayer Ceramic Capacitors: X-Ray Diffractometry and Raman Spectroscopy,” *J. Am. Ceram. Soc.*, **94** [5] 1556–1562 (2011).

[7] D. HENNINGS, A. SCHNELL, and G. SIMON, “Diffuse Ferroelectric Phase Transitions in Ba(Ti1-yZry)O3 Ceramics,” *J. Am. Ceram. Soc.*, **65** [11] 539–544 (1982).

[8] Z. Yu, C. Ang, R. Guo, and A.S. Bhalla, “Piezoelectric and strain properties of Ba(Ti1−xZrx)O3 ceramics,” *J. Appl. Phys.*, **92** [3] 1489–1493 (2002).

[9] T. Maiti, R. Guo, and a. S. Bhalla, “Evaluation of Experimental Resume of BaZr x Ti 1-x O 3 with Perspective to Ferroelectric Relaxor Family: An Overview,” *Ferroelectrics*, **425** [1] 4–26 (2011).

[10] T. Maiti, R. Guo, and A.S. Bhalla, “Structure-Property Phase Diagram of BaZrxTi1−xO3 System,” *J. Am. Ceram. Soc.*, **91** [6] 1769–1780 (2008).

[11] T. Ota, Y. Abe, T. Hirashita, H. Myazaki, Y. Hikichi, and H. Suzuki, “Flat Profile of Permittivity vs Temperature for Graded Ba1-xSrxTiO3 Ceramics,” *J. Ceram. Soc. Japan*, **109** [2] 174–176 (2001).

[12] T. Ota, J. Fujita, S. Kimura, M. Mizutani, Y. Hikichi, H. Myazaki, and H. Suzuki, “Designing of Permittivity vs Temperature Profile for Functionally Graded ƒX PMN-PT,” *J. Ceram. Soc. Japan*, **110** [9] 826–829 (2002).

[13] R.E. Newnham, “Composite electroceramics,” *Ferroelectrics*, **68** [1] 1–32 (1986).

[14] S. Gopalan and A. V Virkar, “Interdiffusion and Kirkcndall Effect in Doped Barium Titanate-Strontium Titanate Diffusion Couples,” *J. Am. Ceram. Soc.*, **78** [4] 993–998 (1995).

[15] S. Gopalan and A. V Virkar, “Interdiffusion and Kirkendall Effect in Doped BaTiO 3 –BaZrO 3 Perovskites: Effect of Vacancy Supersaturation,” *J. Am. Ceram. Soc.*, **82** [10] 2887–2899 (1999).

[16] C.-Y. Siao, H.-W. Lee, and H.-Y. Lu, “Kirkendall porosity in barium titanate–strontium titanate diffusion couple,” *Ceram. Int.*, **35** [7] 2951–2958 (2009).

[17] D. Maurya, N. Wongdamnern, R. Yimnirun, and S. Priya, “Dielectric and ferroelectric response of compositionally graded bilayer and trilayer composites of $BaTiO_3$ and $0.975BaTiO_3–0.025Ba(Cu_{1/3}Nb_{2/3})O_3$,” *J. Appl. Phys.*, **108** [12] 124111 (2010).

[18] M.I.B. Bernardi, E. Antonelli, A.B. Louren, C.A.C. Feitosa, L.J.Q. Maia, and A.C. Hernandes, “$BaTi_{1-x}Zr_xO_3$ NANOPOWDERS PREPARED BY THE MODIFIED PECHINI METHOD,” *J. Therm. Anal. Calorim.*, **87** [3] 725–730 (2007).

[19] T. Sakakibara, H.. Izu, T.. Kura, W.. Shinohara, H.. Iwata, S.. Kiyama, and S. Tsuda, “No Title,” *Proc. IEEE 5th Int. Symp. Micro Mach. Hum. Sci.*, 75 (1994).

[20] S. Sarangi, T. Badapanda, B. Behera, and S. Anwar, “Frequency and temperature dependence dielectric behavior of barium zirconate titanate nanocrystalline powder obtained by mechanochemical synthesis,” *J. Mater. Sci. Mater. Electron.*, **24** [10] 4033–4042 (2013).

[21] N. Sawangwan, J. Barrel, K. MacKenzie, and T. Tunkasiri, “The effect of Zr content on electrical properties of Ba(Ti1-xZrx)O3 ceramics,” *Appl. Phys. A*, **90** [4] 723–727 (2007).

[22] S.J. Kuang, X.G. Tang, L.Y. Li, Y.P. Jiang, and Q.X. Liu, “Influence of Zr dopant on the dielectric properties and Curie temperatures of Ba(ZrxTi1−x)O3 (0≤x≤0.12) ceramics,” *Scr. Mater.*, **61** [1] 68–71 (2009).

[23] S. Mahajan, O.P. Thakur, C. Prakash, and K. Sreenivas, “Effect of Zr on dielectric , ferroelectric and impedance properties of BaTiO 3 ceramic,” *Bull. Mater. Sci.*, **34** [7] 1483–1489 (2011).

[24] W. Li, Z. Xu, R. Chu, P. Fu, and G. Zang, “Dielectric and piezoelectric properties of Ba (Zr x Ti 1 − x) O 3 lead-free ceramics,” *Brazilian J. Phys.*, **40** [3] 353–356 (2010).

[25] F. Moura, a. Z. Simões, B.D. Stojanovic, M. a. Zaghete, E. Longo, and J. a. Varela, “Dielectric and ferroelectric characteristics of barium zirconate titanate ceramics prepared from mixed oxide method,” *J. Alloys Compd.*, **462** [1-2] 129–134 (2008).

[26] L. Dong, D.S. Stone, and R.S. Lakes, “Enhanced dielectric and piezoelectric properties of xBaZrO3-(1−x)BaTiO3 ceramics,” *J. Appl. Phys.*, **111** [8] 084107 (2012).

[27] J. V. Mantese and S.P. Alpay, *GRADED FERROELECTRICS , TRANSPACITORS AND TRANSPONENTS*. Springer, 2005.

[28] R. Bermejo, C. Baudin, R. Moreno, L. Llanes, and A. Sanchezherencia, “Processing optimisation and fracture behaviour of layered ceramic composites with highly compressive layers,” *Compos. Sci. Technol.*, **67** [9] 1930–1938 (2007).

[29] S. Lin, T. Lü, C. Jin, and X. Wang, “Size effect on the dielectric properties of BaTiO3 nanoceramics in a modified Ginsburg-Landau-Devonshire thermodynamic theory,” *Phys. Rev. B*, **74** [13] 134115 (2006).

[30] J.L. Zhu, S. Lin, S.M. Feng, L.J. Wang, Q.Q. Liu, C.Q. Jin, X.H. Wang, C.F. Zhong, *et al.*, "Pressure tuned ferroelectric reentrance in nano-BaTiO3 ceramics," *J. Appl. Phys.*, **112** [12] 124107 (2012).

[31] W. Chaisan, R. Yimnirun, and S. Ananta, "Changes in ferroelectric properties of barium titanate ceramic with compressive stress," *Phys. Scr.*, **T129** 205–208 (2007).

[32] M. Demartin and D. Damjanovic, "Dependence of the direct piezoelectric effect in coarse and fine grain barium titanate ceramics on dynamic and static pressure," *Appl. Phys. Lett.*, **68** [21] 3046 (1996).

[33] T. Sakashita, M. Deluca, S. Yamamoto, H. Chazono, and G. Pezzotti, "Stress dependence of the Raman spectrum of polycrystalline barium titanate in presence of localized domain texture," *J. Appl. Phys.*, **101** [12] 123517 (2007).

[34] T. Hoshina, T. Furuta, T. Yamazaki, H. Takeda, and T. Tsurumi, "Grain Size Effect on Dielectric Properties of Ba (Zr , Ti) O 3 Ceramics," *Jpn. J. Appl. Phys.*, **51** 09LC04–1 (2012).